Proceeding of the IEEE
International Conference on Robotics and Biomimetics (ROBIO)
Shenzhen, China, December 2013

Bezier Curve Based Path Planning for A Mobile Manipulator in Unknown Environments

Jile Jiao, Zhiqiang Cao, Peng Zhao, Xilong Liu and Min Tan

***Abstract*—This paper presents a collision-free path planning approach based on Bezier curve for a mobile manipulator with the endpoints restricted by the manipulator. Based on these candidate endpoints and the initial posture of mobile manipulator, a series of feasible Bezier paths are obtained with the constraints from velocity, acceleration and environment. And then the optimal collision-free path is determined according to the related information of the path as well as obstacles. The mobile manipulator has the ability to adapt to the environment and the optimal path will be updated once the new detected obstacles block this path. The path planning approach is verified by simulations.**

I. Introduction

WITH the expansion of robotic applications, the mobile manipulator operating in unstructured environments is studied extensively. The mobile function and operation function endow the mobile manipulator be applicable both in daily life [1] and in some challenging tasks such as cleaning of hazardous materials, transportation, etc [2]. Yamamoto and Yun present an algorithm to control the mobile platform so that the manipulator is maintained at a configuration which makes the manipulability measure maximum [3]. In [4], Yamamoto and Fukuda investigate multiple mobile manipulators coordinating with each other under a collision avoidance situation, which is verified by simulation. [5] addresses the trajectory tracking problem for a redundantly actuated omnidirectional mobile manipulator with neural network-based sliding mode approach. [6] discusses robotic "assistance" capabilities to aid workers in the accomplishment of a variety of physical operations and presents some control strategies for vehicle-arm coordination, compliant motion tasks, and cooperative manipulation between multiple platforms. Seelinger *et al.* [7] present a high-precision visual control method for mobile manipulators that can maneuver itself into position, engage a target rock, and perform the manipulation tasks, which is demonstrated by experiments. A neural network-based methodology in [8] is developed for the motion control of mobile manipulators subject to kinematic constraints and experimental tests on a 4-DOF manipulator arm illustrate the improved performance of the method. In [9], an approach in control of assembly and disassembly line served by robotic manipulator mounted on mobile platform is represented, which makes the assembly line be reversible. In our earlier work, a vision-based move-to-grasp approach for a compact mobile manipulator is proposed. The visual information of specified object is extracted by two CMOS cameras, and the mobile platform is adjusted based on vision-based control. The effectiveness of the proposed approach is verified by experiments [10].

This paper mainly focuses on path planning problem of the mobile manipulator. For a given object small enough, a grasp circle is determined with its center located at the center of the object, and its radius is chosen according to the structure of the manipulator satisfying that the object can be easily grasped by the mobile manipulator. We may acquire some grasp points distributed on the circle, and they are called the end points. Then the problem is changed into the path planning problem from the starting position of the mobile manipulator to end point.

Path planning is one of the most important problems in mobile manipulator. The path should satisfy the constraints on the vehicle dynamics, and a good path should be safe, smooth, energy saving and adaptive to environments. [11] incorporates path planning problem with image-based control for a wheeled mobile manipulator, and a kinodynamic approach is proposed and demonstrated by experiments. [12] presents a methodology to plan a global path for the gaits of space manipulators with minimum total energy demand, and simulation results show the performance of the algorithm. The path planning of multiple unmanned aerial vehicles based on Bezier curve is addressed in [13]. In [14], a Bezier curve based path planning approach in a robot soccer system is proposed.

Bezier curve is a space curve that is smooth, continuous and derivable [13-15]. In this paper, the Bezier curve based path planning approach is proposed with the constraints of velocity, tangent acceleration as well as obstacles. A serious of feasible Bezier paths can be obtained from the starting point of the mobile manipulator to each end point of the grasp circle. And the optimal collision-free path is determined according to the related information of the path as well as obstacles. Ultrasonic sensors detect obstacles of unknown environment in real-time, and the mobile manipulator will update its path once the new detected obstacles blocks it.

The remainder of the paper is organized as follows. Section II gives the task description. Section III presents the Bezier based collision-free path planning approach. The simulation results are described in section IV and section V concludes the paper.

This work was supported in part by the National Natural Science Foundation of China under Grants 61273352, 61175111, 61227804, 60805038.

Jile Jiao, Zhiqiang Cao, Peng Zhao, Xilong Liu and Min Tan are with the State Key Laboratory of Management and Control for Complex Systems, Institute of Automation, Chinese Academy of Sciences, Beijing 100190, China.
(e-mail: jile.jiao@ia.ac.cn).

II. TASK DESCRIPTION

We denote the starting point of the mobile manipulator as $q_s(x_s, y_s)$, and the object position as $P_t(x_t, y_t)$ (see Fig. 1). The mobile manipulator moves in unknown environment until it arrives at the grasp circle. The grasp circle includes a series of feasible grasp positions $q_e^i(x_e^i, y_e^i)$ (i=1,…,n_e) around the object, where n_e is the number of grasp points. For the safeness of the mobile manipulator and the convenience of path planning, a safety circle is assumed around the mobile manipulator. The safety circle with radius R_r is a circumcircle of the mobile manipulator.

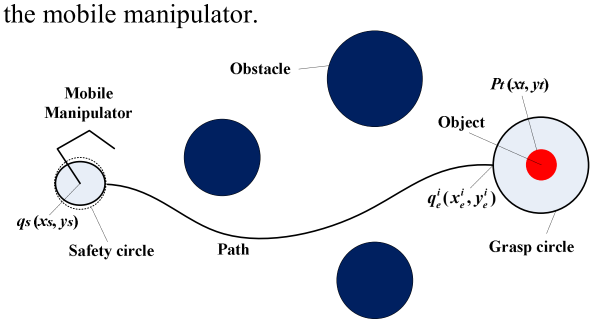

Fig. 1. Task description

A series of Bezier curves may be planned from the initial position q_s to the i^{th} grasp position q_e^i satisfying the following constraints. Note that any a curve should bypass the grasp circle.

1) *Velocity constraint*

Restricted by the mobile manipulator's physical constraints, the speed at any point of its path cannot be higher than its maximal speed V_{max}.

2) *Acceleration constraint*

Restricted by the motor performance, the tangent acceleration a_t along the path cannot larger than the maximal tangent acceleration A_{max}.

3) *Obstacle constraint*

Infeasible regions are those where the mobile manipulator cannot pass through, which are figured out through sensing information and R_r. Therefore the collision-free path should ensure that any point in the path wouldn't enter the infeasible regions.

The optimal one of all feasible paths is chosen based on the evaluations with the consideration of the length and the curvature of the path as well as related information about obstacles. The optimal path will be updated to adapt to the environment according to real-time sensing information.

III. BEZIER CURVE BASED PATH PLAN

A Bezier curve can be represented as

$$P(\tau) = \sum_{i=0}^{n} B_{i,n}(\tau) q_i \quad 0 \le \tau \le 1 \tag{1}$$

where τ is a parameter, $B_{i,n}(\tau) = C_n^{\,i}(I-\tau)^{n-i}\tau^i$ is Bernstein basis polynomials, n is the degree of Bernstein basis, q_i are control points. The polygon drawn through these control points is known as Bezier polygon.

Bezier curves have several useful features for path planning:

1) *Feature of starting point and end point*

According to the definition of Bezier curve, the starting point and the end point on the curve are coincident with the first and the last control points.

2) *Feature of tangent vector*

The derivative of the starting point (τ=0) and the end point (τ=1) of the Bezier curve is

$$q'(0) = n(q_1 - q_0),\ q'(1) = n(q_n - q_{n-1}), \tag{2}$$

which means that the tangent direction of the Bezier curve at starting point and end point coincide with the polygon side q_1q_2 and $q_{n-1}q_n$ (see Fig. 2), respectively.

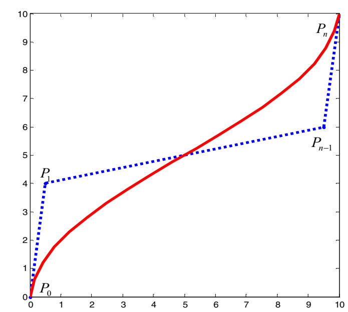

Fig. 2. Bezier curve

3) *Feature of derivative*

The Bezier curve is continuously higher order derivative. A new Bezier curve may be planned from any point of the path to the end point with the tangent direction of this point being unchangeable. Based on this feature, the mobile manipulator can update the path according to the detected environmental information with no abrupt change in path curvature.

A. Cubic Bezier Curve

In this paper, a cubic Bezier curve passing through four control points $q_i(x_i, y_i)$ (i=0,…,3) is adopted. Time is taken as one-dimensional variable to the solution model. t_i(i=0,…,3) is the time of four control points.

The cubic Bezier curve is given by

$$\begin{cases} x(\tau) = \sum_{i=0}^{3} B_{i,n}(\tau) q_i = x_0(1-\tau)^3 + 3x_1\tau(1-\tau)^2 + 3x_2\tau^2(1-\tau) + x_3\tau^3 \\ y(\tau) = \sum_{i=0}^{3} B_{i,n}(\tau) q_i = y_0(1-\tau)^3 + 3y_1\tau(1-\tau)^2 + 3y_2\tau^2(1-\tau) + y_3\tau^3 \\ t(\tau) = \sum_{i=0}^{3} B_{i,n}(\tau) q_i = t_0(1-\tau)^3 + 3t_1\tau(1-\tau)^2 + 3t_2\tau^2(1-\tau) + t_3\tau^3 \end{cases} \tag{3}$$

Equation (3) can be expanded and rearranged to the form of a third order polynomials about τ as

$$\begin{cases} x(\tau) = a_0 + a_1\tau + a_2\tau^2 + a_3\tau^3 \\ y(\tau) = b_0 + b_1\tau + b_2\tau^2 + b_3\tau^3 \\ t(\tau) = c_0 + c_1\tau + c_2\tau^2 + c_3\tau^3 \end{cases} \tag{4}$$

where a_i, b_i, c_i (i=0,…,3) are coefficients of Bezier curve which can be evaluated in terms of the four control points.

B. Selection of Control Points

According to the feature of starting point and end point, the first control point is the starting point q_s of the mobile manipulator with the direction of velocity pointing at P_t. t_0=0 is the starting time, ($\dot{x}_s, \dot{y}_s$) is the starting velocity.

1) *The fourth control point*

The fourth control point is one of end points with its direction of velocity pointing at P_t. In this paper, the radius of the grasp circle is defined according to the maximum and minimum lengths l_m, l_n of the manipulator arm when grasping. The kinematic model of the 3-DOF manipulator is given as

$$\begin{cases} h = l_3\sin\theta_3 + l_2\sin(\theta_2+\theta_3) + l_1\sin(\theta_1+\theta_2+\theta_3) + h_r \\ l = l_3\cos\theta_3 + l_2\cos(\theta_2+\theta_3) + l_1\cos(\theta_1+\theta_2+\theta_3) \end{cases}. \quad (5)$$

where h_r is the installation height of the manipulator, l_1, l_2 and l_3 are the lengths of the connecting rods, θ_1□$[0, \pi]$, θ_2□$[-\pi/2, \pi/2]$ and θ_3□$[-\pi/2, \pi/2]$ are the wrist joint, the elbow joint and the shoulder joint of the manipulator, respectively.

Suppose that the height of grasp point to the ground is h_e, all possible angle combinations are scanned to obtain the maximum and minimum length of the manipulator, that is, $l_m=\max(l)|h=h_e$, $l_n=\min(l)|h=h_e$. A proper radius of the grasp circle $l_e=(l_m+l_n)/2$ is chosen, which is shown in Fig. 3.

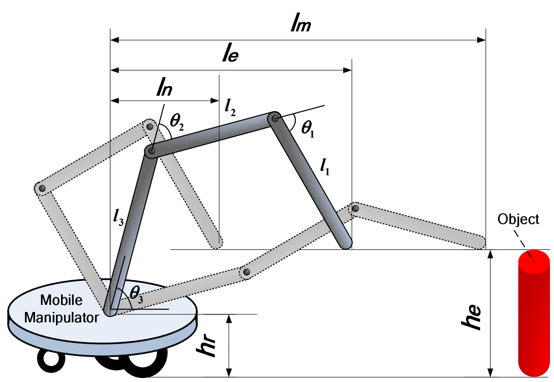

Fig. 3. The radius of grasp circle

Thus, the position of end point i is represented as

$$\begin{cases} x_e^i = x_t + l_e\cos\phi_i \\ y_e^i = y_t + l_e\sin\phi_i \end{cases} \quad (\phi_i = \Delta\vartheta k_e, k_e = 1,\ldots,n_e) \quad (6)$$

where $\Delta\vartheta = 2\pi/n_e$ is the angle interval between the adjacent end points. In addition, t_3 is given based on the straight-line distance and the initial velocity v_0 of the mobile manipulator.

$$t_3 = \sqrt{(x_s-x_t)^2+(y_s-y_t)^2} \Big/ v_0 \quad (7)$$

2) *Selection of the second and the third control points*

According to the feature of tangent vector of Bezier curve, it is obvious that the second/third control point is on the direction of velocity of the first/fourth control point.

The parameters of the first control point and the fourth control point are expressed as $P_0(x_s, y_s, t_0)$ and $P_3(x_e^i, y_e^i, t_3)$, respectively. There are $N_i=t_3/T_s$ Bezier curves planned from P_0 to P_3, where T_s is the sample time. Parameters of the second control point and the third control point of the u^{th} ($u=1,\ldots,N_i$) Bezier path are expressed as

$$P_1(x_s + u\Delta d_s\dot{x}_s, y_s + u\Delta d_s\dot{y}_s, u\Delta d_s/v_0) \quad (8)$$

$$P_2(x_e^i - u\Delta d_e\dot{x}_e^i, y_e^i - u\Delta d_e\dot{y}_e^i, t_3 - u\Delta d_e/v_3) \quad (9)$$

where $v_3=v_0$, Δd_s and Δd_e are given lengths and they are defined as

$$\Delta d_e = \sqrt{(x_s-x_t)^2+(y_s-y_t)^2} \Big/ N_i \quad (10)$$

$$\Delta d_s = \Delta d_e/4 \quad (11)$$

C. Constraints

As discussed in section II, the mobile manipulator constraints as well as obstacles should be considered during path planning.

1) *Constraints of mobile manipulator*

Restricted by the physical constraints of mobile manipulator and the performance of the motor, the velocity and tangent acceleration of the mobile manipulator at any time must satisfy their constraints.

The velocity and tangent acceleration of each sample point are figured out. Based on the continuity and differentiability of Bezier curve, the first derivative of x, y and t to parameter τ are as follows.

$$\begin{aligned} \dot{x} &= dx(\tau)/d\tau = 3a_3\tau^2 + 2a_2\tau + a_1 \\ \dot{y} &= dy(\tau)/d\tau = 3b_3\tau^2 + 2b_2\tau + b_1, \\ \dot{t} &= dt(\tau)/d\tau = 3c_3\tau^2 + 2c_2\tau + c_1 \end{aligned} \quad (12)$$

Hence, the velocity can be solved by $v = \sqrt{v_x^2 + v_y^2}$, where $v_x = \dot{x}/\dot{t}$, $v_y = \dot{y}/\dot{t}$. Furthermore,

$$\begin{aligned} \ddot{x} &= d^2x(\tau)/d\tau^2 = 6a_3\tau + 2a_2 \\ \ddot{y} &= d^2y(\tau)/d\tau^2 = 6b_3\tau + 2b_2\tau \end{aligned}. \quad (13)$$

The tangent acceleration is given by

$$a_t = v^2 \times \kappa. \quad (14)$$

where the curvature of Bezier curve is defined as $\kappa = \dfrac{|\dot{x}\ddot{y} - \ddot{x}\dot{y}|}{(\dot{x}^2+\dot{y}^2)^{3/2}}$.

All sample points of feasible path should satisfy $v \le V_{max}$ and $a_t \le A_{max}$.

2) *Obstacles constraint*

There are k_s ultrasonic sensors and we assume that there is no overlapping region between two non-adjacent sensors. The axis angle of sensor $S_k(k=1,\ldots,k_s)$ is $\varphi_s^k=-\pi/2+(k-1)\pi/(k_s-1)$ with respect to the moving direction of mobile manipulator. Each sensor is capable of detecting the angle range of A_g with a distance range D_e. Denote ρ_s^k as the returned data of sensor k, ρ_s^k is the distance between the sensor and the obstacle when an obstacle is detected, otherwise, $\rho_s^k=D_e$.

It is obvious that the more precise the obstacle is detected, the better the path is planned. According to A_g and k_s, we may subdivide the regions of ultrasonic sensors. If $A_g \le \pi/(k_s-1)$, there are $R_v(v=1,\ldots,k_s)$ regions corresponding to the regions of the sensors and $\eta_R^v=\rho_s^k$, or else, the adjacent sensors have overlapping regions. In this case, these regions are subdivided into sub-regions $R_v(v=1,\ldots,2k_s-1)$, and η_R^v is given as follows.

$$\eta_R^v = \begin{cases} \rho_s^k & v = 2k-1, k = 1,\ldots,k_s \\ \max(\rho_s^k, \rho_s^{k+1}) & v = 2k, k = 1,\ldots,k_s-1 \end{cases} \quad (15)$$

If there is an obstacle in region R_v, there exists infeasible region considering the safety circle, which is shown as Fig. 4. Point P_n in the infeasible region should satisfy the following conditions:

$$\theta_n \ge \theta_l^v \;\&\&\; \theta_n \le \theta_r^v \;\&\&\; D_n \ge (\eta_R^v - R_r) \;\&\&\; D_n \le (\eta_R^v + R_r) \quad (16)$$

where Q_r is the intersection point of two lines L_l and L_r extended outside R_r from two boundaries of region R_v; θ_n is the angle between the line from Q_r to P_n and the horizontal direction; θ_l^v and θ_r^v are angles between L_l/L_r and the horizontal direction, respectively; D_n is the distance between P_n and the present position of mobile manipulator.

According to the information of all R_v with the consideration of impassability of the grasp circle, a series of infeasible regions are obtained. Then those Bezier paths that pass through any an infeasible region will be removed. Fig. 4 shows an example of a feasible path.

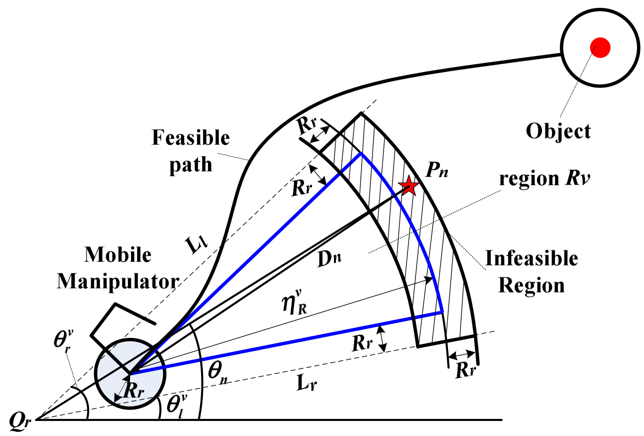

Fig. 4. Infeasible region and feasible Bezier path

D. Optimal Path

All feasible Bezier paths consist of the set Ω_f. Evaluate the path L in Ω_f using the length and curvature of the path:

$$V_L = k_1\int_0^1 \sqrt{x(\tau)^2 + y(\tau)^2}\,d\tau + k_2\int_0^1 \kappa(\tau)\,d\tau \quad (L \in \Omega_f) \quad (17)$$

where k_1 is the weight of path length, and k_2 is the weight of curvature of the path.

Generally, the shorter path with lower curvature is preferable with the consideration of efficiency and smoothness. Also, limited by the sensing range, more sensing information caused by an obstacle may be obtained step by step, which makes the path being very close to an obstacle become infeasible easily. Therefore, the minimum distance D_m^L between infeasible regions and path points near the obstacles should be an important factor when choosing the optimal path.

The optimal path L_o can be represented as

$$L_o = \min_{L \in \Omega_l}(V_L) \quad (18)$$

where Ω_l is the set of paths in Ω_f satisfying $D_m^L > T_D$, or else, it is equivalent to Ω_f; T_D is a given threshold.

E. Bezier Path Update

As mentioned above, the sensing information changes in real-time with the mobile manipulator moving along the planned path. Whenever the mobile manipulator thinks its path passes through any an infeasible region, it has to update the path based on the present position and velocity.

An example of path update is shown in Fig. 5. At the beginning, the ultrasonic sensors can only detect infeasible region 1, and path 1 is chosen as an optimal path, however, when the mobile manipulator is at point P_u, infeasible region 2 is detected, so the mobile manipulator plan its path again and choose the path 2 to move.

When the mobile manipulator finally arrives at the grasp circle, its arm grasps the object based on the inverse kinematics.

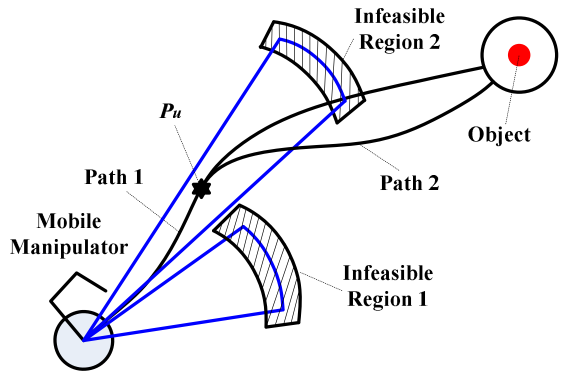

Fig. 5. Bezier Path update

IV. Simulation Results

To testify the proposed approach, several simulation experiments have been carried out. The mobile manipulator parameters are given as follows. V_{max}=0.4 m/s, A_{max}= 0.1 m/s^2, R_r=0.2 m, h_r=0.108 m, l_1=0.16 m, l_2=0.16 m, l_3=0.2 m, θ_1= –0.8 rad, θ_2= –1.5 rad, θ_3=2.2 rad, k_s=5, A_g=1.05 rad, D_e=2.5 m. The object parameter is given as h_e=0.208m. The algorithm parameters are n_e=36, v_0=0.2m/s, T_s=0.5 s, k_1=0.8, k_2=0.2, T_D=15.

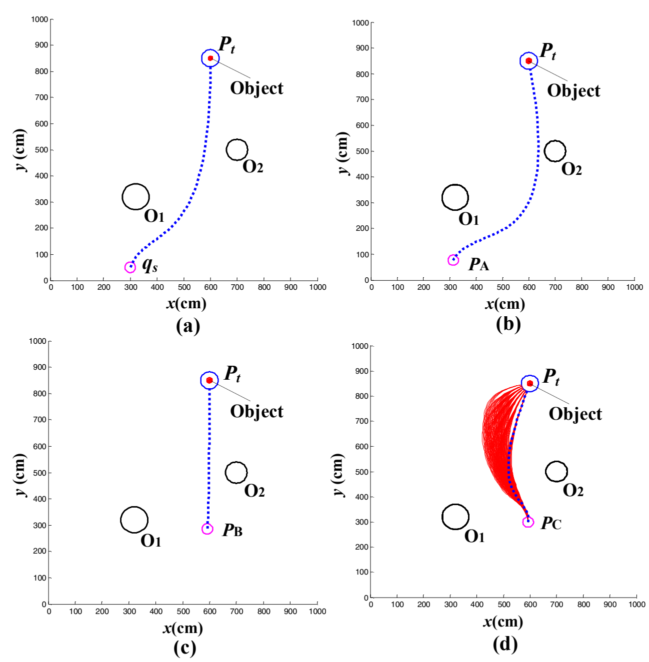

Fig. 6. The optimal paths of different positions in simulation experiment 1

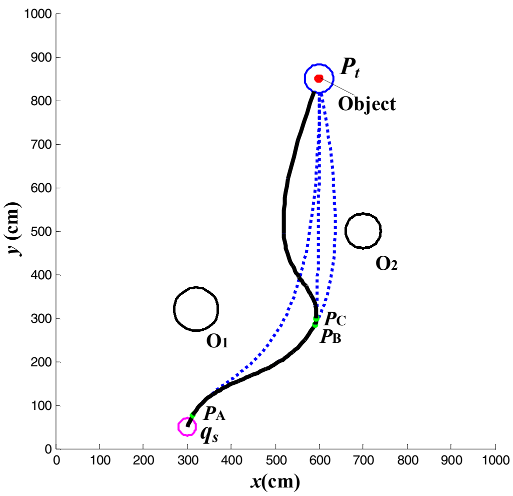

Fig. 7. Trajectory of the mobile manipulator of simulation experiment 1

In simulation experiment 1, the starting point of mobile manipulator is q_s, and the object position is P_t. Fig. 6 gives the optimal paths of different positions, which are drawn in blue dotted lines. The trajectory of the mobile manipulator is depicted in Fig. 7. The optimal path from starting point q_s is shown as Fig. 6(a). When the mobile manipulator moves to point P_A in Fig. 6(b), the obstacle O_1 blocks the path, and the mobile manipulator makes its change. Similarly, the mobile manipulator changes its paths at point P_B (see Fig. 6(c)) and P_C (Fig. 6(d)) because of obstacle O_2. The red lines in Fig. 6(d) show all feasible paths from point P_C to end points.

Fig. 8 gives another simulation result in a different environment. As shown in Fig. 8, constrained by the environment, the path is updated seven times for mobile manipulator. From the above simulation results, the proposed approach may achieve the collision-free planning of the mobile manipulator with the ability to adapt to the environment.

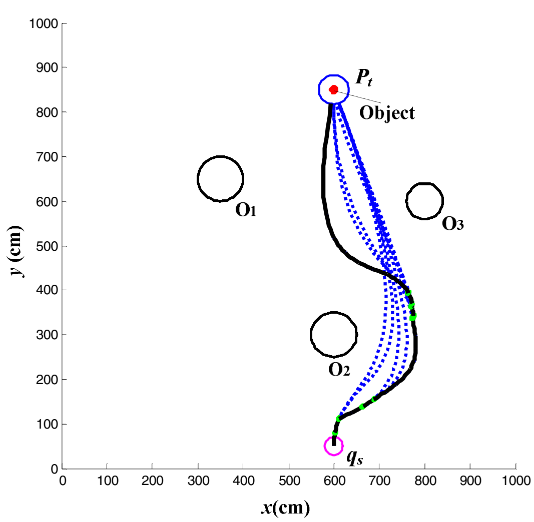

Fig. 8. Trajectory the mobile manipulator of simulation experiment 2

V. Conclusion

In this paper, we present a collision-free path planning approach for the mobile manipulator based on Bezier curves. The constraints of velocity, the tangential acceleration and obstacles are considered during the path planning. Simulation results show that the Bezier curve based path planning may guide the mobile manipulator to approach the object smoothly without collisions with environmental obstacles.

References

[1] A. Jain and C. C. Kemp, "EL-E: An Assistive Mobile Manipulator that Autonomously Fetches Objects from Flat Surfaces," *Autonomous Robots*, vol. 28, no. 1, pp. 45-64, 2010.

[2] Y. Wang, H. X. Lang and C. W. de Silva, "A Hybrid Visual Servo Controller for Robust Grasping by Wheeled Mobile Robots," *IEEE Transactions on Mechatronics*, vol. 15, no. 5, pp. 757-769, 2010.

[3] Y. Yamamoto and X. P. Yun, "Coordinating Locomotion and Manipulation of a Mobile Manipulator," *IEEE Transactions on Automatic Control*, vol. 39, no. 6, pp. 1326-1332, 1994.

[4] Y. Yamamoto and S. Fukuda, "Trajectory Planning of Multiple Mobile Manipulators with Collision Avoidance Capability," *Proceedings of the International Conference on Robotics and Automation*, Washington DC, pp. 3565-3570, 2002.

[5] D. Xu, D. B. Zhao, J. Q. Yi and X. M. Tan, "Trajectory Tracking Control of Omnidirectional Wheeled Mobile Manipulator: Robust Neural Network-Based Sliding Mode Approach," *IEEE Transactions on Systems, Man and Cybernetics, Part B: Cybernetics*, vol. 39, no. 3, pp. 788-799, 2009.

[6] O. Khatib, "Mobile manipulation: The robotic assistant," *Robotics and Autonomous System*, vol. 26, pp. 175-183, 1999.

[7] M. Seelinger, J. D. Yoder, E. T. Baumgarter and S. B. Skaar, "High-Precision Visual Control of Mobile Manipulators," *IEEE Transactions on Robotics and Automation*, vol. 18, no. 6, pp. 957-965, 2002.

[8] L. Sheng and A. A. Goldenberg, "Neural-Network Control of Mobile Manipulators," *IEEE Transactions on Neural Networks*, vol. 12, no. 5, pp. 1121-1133, 2001.

[9] E. Minca, A. Filipescu and A. Voda, "New approach in control of assembly/disassembly line served by robotic manipulator mounted on mobile platform ," *Proceedings of the 2012 IEEE International Conference on Robotics and Biomimetics*, Guangzhou, China, pp. 235-240, 2012.

[10] J. Jiao, S. Ye, Z. Cao, N. Gu, X. Liu and M. Tan, "Embedded Vision Based Autonomous Move-to-Grasp for Mobile Manipulator", *International Journal of Advanced Robotic Systems*, vol. 9, 2012

[11] M. Kazemi, K. Gupta and M. Mehrandezh, "Path planning for image-based control of wheeled mobile manipulators," *IEEE/RSJ International Conference on Intelligent Robots and Systems*, Vilamoura, Algarve, Portugal, pp. 5306-5312, 2012.

[12] K. C. Wing and Y. S. Xu, "Path planning algorithm for space manipulator with a minimum energy demand," *Proceedings of the 2012 IEEE International Conference on Robotics and Biomimetics*, Guangzhou, China, pp. 1556-1563, 2012.

[13] F. Hu and S. Wang, "An algorithm for path planning of multiple unmanned aerial vehicles based on Bezier curve", *Proceedings of the 29th Chinese Control Conference*, Beijing, China, pp. 3660-3665, 2010.

[14] K. G. Jolly, R. Sreerama Kumar and R. Vijayakumar, "A Bezier curve based path planning in a multi-agent robot soccer system without violating the acceleration limits," *Robotics and Autonomous Systems*, vol. 57, no. 1, pp. 23-33, 2009.

[15] H. Long, H. Yashiro, H. T. N. Nejad, H. D. Quoc and M. Seiichi, "Bézier curve based path planning for autonomous vehicle in urban environment," *IEEE Intelligent Vehicles Symposium*, San Diego, CA, USA, pp. 1036-1042, 2010.